The role of asymmetric prediction losses in smart charging of electric vehicles

Milan Straka[1,2], Ľuboš Buzna[1], Nazir Refa[3], and Santiago Mazuelas[2]

[1] *University of Žilina, Univerzitná 8215/1, Žilina, Slovakia*
[2] *BCAM-Basque Center for Applied Mathematics, 48009 Bilbao, Spain*
[3] *ElaadNL, Utrechtseweg 310 (bld. 42B), 6812 AR Arnhem (GL), The Netherlands*

Abstract

Climate change prompts humanity to look for decarbonisation opportunities, and a viable option is to supply electric vehicles with renewable energy. The stochastic nature of charging demand and renewable generation requires intelligent charging driven by predictions of charging behaviour. The conventional prediction models of charging behaviour usually minimise the quadratic loss function. Moreover, the adequacy of predictions is almost solely evaluated by accuracy measures, disregarding the consequences of prediction losses in an application context. Here, we study the role of asymmetric prediction losses which enable balancing the over- and under-predictions and adjust predictions to smart charging algorithms. Using the main classes of machine learning methods, we trained prediction models of the connection duration and compared their performance for various asymmetries of the loss function. In addition, we proposed a methodological approach to quantify the consequences of prediction losses on the performance of selected archetypal smart charging schemes. In concrete situations, we demonstrated that an appropriately selected degree of the loss function asymmetry is crucial as it almost doubles the price range where the smart charging is beneficial, and increases the extent to which the charging demand is satisfied up to 40%. Additionally, the proposed methods improve charging fairness since the distribution of unmet charging demand across vehicles becomes more homogeneous.

Keywords

machine learning, asymmetric loss function, smart charging, electric vehicles

List of symbols

- N - number of observations in the training set,

- P - number of features in the training set,

- M - number of layers in the neural network,

- T - number of observations in the test set,

- $M^{(i)}$ - number of neurons that compose i-th layer of a neural network,

- $J^{(i)}$ - number of leaf nodes of the i-th regression tree,

- r - residual,

- r_i - residual associated with i-th observation,

- a, b - parameters of the linear-linear loss function,

- $\rho(r)$ - loss function,

- y_i - target variable (representing the connection duration),

- x_{ij} - i-th observation of the j-th feature,

1

- $\boldsymbol{x}$ - vector of feature values associated with one observation,

- $\boldsymbol{x}_k$ - vector of feature values associated with one k-th observation,

- β_0 - intercept in the regression model,

- β_j - regression coefficient corresponding to the j-th feature,

- λ, α - hyperparameters used for the regularisation of the loss function,

- $f^{(i)}(\boldsymbol{x})$ - prediction of the target variable for $\boldsymbol{x}$, provided by the GBRT at the i-th iteration,

- $R_j^{(i)}$ - domain of the j-th leaf node of the i-th regression tree,

- $\omega_j^{(i)}$ - real value assigned to the domain of the j-th leaf node of the i-th regression tree during the training process,

- $g(\boldsymbol{x})$ - function modelling the output of the neural network,

- $g^{(i)}$ - function modelling the output of the i-th layer of the neural network,

- $g_k^{(i)}$ - function modelling the output of the k-th neuron at the i-th layer of the neural network,

- $s(.)$ - activation function applied by a neural network,

- $\gamma_{jk}^{(i)}$ - weight of the connection between j-th neuron from the i-th layer and k-th neuron from the $i+1$-th layer

- $\gamma_{0k}^{(i)}$ - weight representing the constant term in the linear combination processed by k-th neuron at i-th layer

- t_i^{arr} - observed arrival time of a vehicle to a charging station,

- t_i^{dep} - observed departure time of a vehicle from a charging station,

- t_i^{char} - time when a charging of a vehicle was terminated,

- $\hat{t}_i^{dep}$ - estimated departure time of a vehicle from a charging station,

- P^{BaU} - constant value of charging power applied by the business-as-usual charging scheme,

- P^{UP} - constant value of charging power applied by the uniform power charging scheme,

- E^p - the energy charged in the peak price period (if a subscript i is added it refers to the i-th charging session),

- E^o - the energy charged in the off-peak price period (if a subscript i is added it refers to the i-th charging session),

- E^n - energy that could not be charged by a smart charging scheme due to the misestimate of the connection duration (if a subscript i is added it refers to the i-th charging session),

- E^a - the energy charged by the uniform power charging scheme at the higher value of power than is the power applied by the business-as-usual charging strategy (if a subscript i is added it refers to the i-th charging session),

- E^s - the energy charged by the uniform power charging scheme at the smaller value of power than is the power applied by the business-as-usual charging strategy (if a subscript i is added it refers to the i-th charging session),

- E^l - overall energy charged by the uniform power charging scheme at higher or lower rate than energy charged by the business-as-usual charging scheme,

- w^o - unit costs associated with E^o,

- w^p - unit costs associated with E^p,

- w^n - unit costs associated with E^n,

- w^l - unit costs associated with E^l.

1 Introduction

1.1 Motivation

Recent climate report [1] reaffirms with high confidence a relationship between anthropogenic CO_2 emissions and the increasing average Earth surface temperature, which is likely to hamper the quality of human life on a global scale in the next decades. Electric vehicles (EVs) are superior to internal combustion engine vehicles for reducing oil use and local air pollution. The energy and environmental benefits of EV introduction are safe to claim if EVs are dominantly charged from renewable energy sources [2]. The market share of EVs continues to grow. However, several challenges must be addressed: supply chain environment (chip and battery shortages, reliance on rare materials), availability of convenient and affordable charging infrastructure and customer acceptance. The positive environmental impacts of EVs can be augmented by adequately coordinating the EV charging with the presence of electricity generated from renewable energy sources [3]. For example, the household photovoltaics can meet 56% of EVs electricity requirements and with coordinated charging it can be increased to 90% [4]. Additionally, coordinated EV charging can bring benefits to EV drivers, e.g., by shifting the charging to times with smaller charging prices, as well as charging infrastructure operators, e.g., by decreasing transformer ageing [5] and by increasing up to ten times the number of charging stations that can be installed on the same grid [6]. Renewable energy sources also bring considerable challenges. The variability of wind and solar requires balancing the supply and demand on different time scales. Their distributed nature makes difficult connecting them to the existing grid infrastructure. These aspects have implications for electricity markets, regulation and governance procedures. To exploit the available renewable energy sources and to provide profitable services, the coordinated EV charging must be operated from the future perspective. Therefore, charging control algorithms take advantage of predictions made based on past operational data. In the scientific literature, EV charging predictions have been often developed in isolation from charging algorithms. Consequently, the potential to optimise the performance of a charging scheme by adjusting the properties of predictions has not been fully analysed yet. A natural way to achieve this goal is to adjust the loss function associated with the prediction method. The loss function maps the difference between an observed value of the predicted quantity and its estimate provided by the model to the quantity (called prediction loss or error) that is minimised by the training process to determine the model parameters. Thus, the shape of the loss function can influence the frequency and size of under- and over-predictions of the output variable. For a smart charging scheme, the over-prediction of the charging duration creates false expectations about the possibility to postpone the EV charging that may result in an insufficient state of battery charge. On the contrary, the under-prediction can lead to a higher price of charging or lower utilisation of renewable energy due to missing the opportunity to postpone the EV charging. In this paper, we show that by suitably modulating the loss function we can significantly improve the performance and profitability of EV charging coordination schemes.

1.2 Terminology

Across the paper, we use several specific terms that we define in this section.

- *Charging point* is an energy delivery device that might have one or several connectors, where only one can be used at the same time to charge an EV.

- *Charging station* is an object with one or more charging points that share a common driver identification interface [7].

- *Charging session*, often referred to as a charging transaction, is an EV charging action that starts by plugging a vehicle into a charging station and ends by unplugging it out.

- *Connection duration* is the duration of a charging session.

- *Charging duration* is the part of the connection duration, when energy is transferred from a charging station to a vehicle.

- *Smart charging* is any type of optimised and coordinated charging of EVs [7]. For example, Hoed et al. [8] define smart charging as optimising the execution of a charging session in time, speed and direction of charging.

1.3 Literature review

In the following we describe smart charging schemes while focusing on required inputs. Next, we provide an overview of EV charging datasets. Further, we discuss the prediction problems in the EV charging domain, followed by an overview of the prediction methods used. Finally, we briefly overview asymmetric loss functions and their applications.

1.3.1 Smart charging

The EV charging profiles directly affect the loading of the power grid network. When EV charging is uncoordinated (uncontrolled), the batteries of the EVs either start charging when an EV is plugged in or after a user-adjustable fixed start delay [9]. As most EVs arrive at work or home at a similar time, they could create a large load coincident with the peak. The situation can be improved by coordinated charging when EVs are preferably charged during the off-peak period. The interaction between EVs and the smart grid is implemented through aggregators representing EV charging infrastructure, including power network substations and parking lots [10]. The information exchange between the smart grid and EVs is through communication networks. The power and communication networks together compose a complicated system that needs efficient control strategies.

Various types of smart charging algorithms have been proposed to implement coordinated charging. A review of smart charging algorithms in [10] classified the algorithms into three categories: smart grid oriented, aggregator oriented and driver-oriented. Another review of smart charging algorithms [11] highlights as possible future directions the development of prediction methods that are able to deal with uncertainty in driver mobility behaviour and the development of approaches properly balancing prediction accuracy, model simplicity, and data requirements. Smart charging schemes follow various optimisation objectives including the minimisation of charging cost [12, 13, 14, 15] and peak power minimisation [12, 13, 14]. Less common approaches aim to minimise transformer [12] and battery ageing [16], to maximise utilisation of renewable resources [11, 17] or to combine these criteria [12].

The EV charging flexibility is the extent to which the charging can be coordinated [17]. Some studies evaluate the charging flexibility on historical charging data. In [17], the authors provide a complex analysis of the EV charging flexibility by comparing two strategies, the peak flattening and the maximisation of renewable energy usage. In another study [14], authors estimated the benefits of non-residential smart charging on two scenarios. In the first scenario, behind-the-meter EV aggregations are combined with the time-of-use (ToU) smart charging scheme while in the second scenario the spatial aggregation is combined with the minimisation of the peak load. Both case studies resulted in significant monetary savings and peak power decrease.

Another approach to EV charging flexibility concerns the willingness of EV drivers to change their charging habits. In [6], the authors described a smart charging experiment where EV drivers were incentivised to use a mobile phone app to cancel or change the speed of charging. The experiments showed that drivers are willing to adapt to the system requirements. However, the mobile app usage decreased to 2-3% of all sessions after a few weeks. Zweistra et al. [18] performed a smart charging experiment to decrease the peak load. The authors evaluated the number of sessions that were terminated before the charging was completed. The number of such sessions was surprisingly low, confirming the potential benefits of smart charging. The importance of a sufficient state of charge (SoC) was confirmed by surveying early EV adopters, indicating problems with the acceptance of smart charging if it would negatively impact their mobility [19].

Smart charging algorithms exploit charging flexibility to reschedule the charging sessions and obtain a favourable electricity consumption profile. A possible approach resides in distributing the EV charging over the entire connection duration. The connection duration is unknown at the time when an EV is plugged into the charging station; hence, it must be estimated. The loss function is an essential component of the prediction methods, directly impacting the distribution of estimation losses. The distribution of estimation losses impacts the performance of smart charging algorithms in a nontrivial way. This paper investigates how the used loss function affects the performance of selected smart charging schemes.

1.3.2 Prediction problems

The most often the smart charging applications rely on point predictions of energy time series [20, 21]. Recently, the probabilistic forecasts were applied to capture the stochastic load induced by EV charging [22, 23, 24, 25]. Such forecasts can inform the smart charging algorithms at a spatially aggregated

scale. For the local management were developed predictions of charging station occupancy [26, 27] and day ahead charging probabilities for individual EVs [28] in the form of time series.

Smart charging schemes are mostly dependent on parameters that locally describe EV drivers' behaviour. For example, such parameters are the number of EVs charging in a given time interval [29], or charging session attributes such as arrival time [12], departure time, connection duration, charging duration, and energy demand [14, 30, 17]. Prediction models of connection duration and charged energy were proposed in [31] using ensemble models. An alternative approach is to ask EV drivers about the planned departure time at the time when they initiate the charging [32]. However, the accuracy of driver estimates was found to be smaller than of estimates provided by machine learning methods [33].

A review [34] of EV charging prediction approaches states that the fundamental problem of many studies is a limited accuracy of arrival and departure time models, questioning their real-world applicability. This might be connected with the fact, that many of the previously mentioned studies evaluate the predictions by the accuracy measures, without checking if they satisfy the needs arising from applications. In [33], authors predicted energy demand and charging duration, considering work charging and applied them to study possibilities of load curve smoothing. This work was extended in [35] and [36], while improving the accuracy of predictions. Frendo et al. [37] made predictions of EV departure times using regression models trained on historical work charging data. The predictions were verified on smart charging schemes. Another interesting real-world application of connection duration predictions is optimising the charging energy profile to minimise the battery degradation [32].

1.3.3 Prediction methods and EV charging datasets

There is a broad range of machine learning applications in the EV field, mostly utilising supervised learning methods. A comprehensive review of machine learning approaches to analyse and predict the EV charging behaviour can be found in [38]. Examples include logistic regression [28], general logistic models [26], Gaussian mixture models [33], and support vector regression [39, 40]. Among the best performing machine learning methods are the decision tree methods. The following were applied to predict the EV charging behaviour: random forest [41, 39], XGBoost [41, 37], gradient boosting machines [41], and Light gradient boosting [32]. Decision tree-like methods are also the most utilised methods by ensemble approaches [42, 31, 43]. Numerous studies also applied artificial neural networks to predict EV charging behaviour [41, 36, 27, 37], long short-term memory networks [21] as well as quantile neural networks [23]. Ensemble approaches combine prediction methods, e.g., [36] combined support vector machines, random forest, deep neural network, and XGBoost into voting and stacking ensemble. In recent years, reinforcement learning methods gained on popularity. A review of these approaches with applications in the EV charging management is provided in [44]. Such approaches can be superior to deep learning in predicting the charging load [45].

The performance of machine learning methods is strongly dependent on available data. The first EV charging data were brought by small pilot projects [46]. In recent years, the growing adoption of EVs resulted in several publicly available EV charging datasets, allowing researchers to study EV charging behaviour. A comprehensive review of EV charging datasets is provided in [47]. Based on the types of charging behaviour, we distinguish home, work, or mixed EV charging datasets. Mixed datasets are more heterogeneous and hence more challenging to predict. One of the largest publicly available datasets is the "Electric Chargepoint Analysis: Domestics" [32]. It is a home charging dataset covering approximately 25 000 households in the UK. A work charging dataset [37] describes EV charging taking place on several parking lots located in German cities. In [39] is presented one of the few datasets containing state of charge data. In [48] authors analysed smart charging data, containing also SoC at arrival. The popular ACN dataset [33] consists of two work charging datasets: JPL and Caltech. The Dundee dataset [27] is of the mixed type as offers 67 000 records from fast and rapid charging stations. For the numerical experiments, we use the EVnetNL dataset [23] that is one of the most frequently studied mixed charging datasets encompassing a large time span and wide geographical coverage. The EVnetNL dataset is further detailed in Section 3.1.

1.3.4 Asymmetric loss functions

A loss function is a tool to evaluate how well the prediction model fits the data. It takes as an argument the current output of the prediction method and the expected output and returns a value to be minimised during the learning process. Such value is a feedback signal to adjust the prediction model parameter

values. If the values returned by a loss function are symmetric with respect to the zero distance between the prediction method and its expected output, the under- and over-estimates of predicted quantity are treated equally. In the energy field, publications rarely consider asymmetric loss functions. A modification of the support vector regression method that includes a linear asymmetric loss function for electric load forecasting was developed in [49]. The use of asymmetric loss function was motivated by different financial costs resulting from over-and under-estimates of the electricity load. In the EV charging domain, we identified only two studies utilising an asymmetric loss function. Kim et al. [50] proposed a discrete choice model with linear asymmetric loss function. The model captures EV buying decisions based on consumption preferences. The second study [51] developed predictions of time series of charged and discharged electric energy resulting from the operation of a fleet of shared EVs. The asymmetric loss function models the higher income losses when an EV cannot be rented due to low SoC, as when not using an opportunity to sell the energy stored in the EV battery to the grid.

1.4   Contribution and structure of the paper

Smart charging algorithms require estimates of future charging demand. Available prediction models of a charging behaviour usually minimise the quadratic loss function. Thus, the frequency and amplitude of over- and underestimations are not optimised to the requirements of a smart charging scheme. We deliver three main contributions:

- We demonstrate the benefits of modulating the loss function and this way optimising the consequences of over- and underestimation for smart charging schemes.

- We propose a methodological approach to quantify the uneven consequences of predictions on the performance of selected archetypal smart charging schemes.

- We provide an interpretation of implications of conducted analysis for real-world EV charging systems.

To the best of our knowledge, this is the first paper evaluating the benefits of cost-sensitive predictions (i.e. predictions that account for the fact that under- and over-predictions have unequal consequences for a smart charging scheme) [52].

The rest of the paper is organised as follows. Section 2 introduces asymmetric loss functions, prediction methods, features, evaluation procedure, considered smart charging schemes, data processing and implementation settings. Used dataset, data analysis, comparison of prediction methods and study of the impact of cost-sensitive predictions on the smart charging schemes are documented in Section 3. Summary of conclusions, limitations, and future outlooks are provided in Section 4.

2   Methods

The section starts with the background information. We review briefly the concept of the asymmetric loss function (Section 2.1), used prediction methods (Section 2.2), variables selected to create prediction models (Section 2.3), performance measures used to evaluate the accuracy of prediction models (Section 2.4), and selected smart charging schemes (Section 2.5). The section concludes by describing the methodology proposed by the authors. In Section 2.6 is introduced the methodology to assess the impact of under- and over-estimation of the connection duration on the performance of smart charging schemes. Section 2.7 describes the methodology to process the data and how is the data used to train and validate prediction models. Finally, Section 2.8 delineates the setting of model parameters.

2.1   Asymmetric loss functions

We utilize a piecewise-linear loss function (see Figure 1) that can be described as

$$\rho(r) = \begin{cases} br \text{ if } r \leq 0 \\ ar \text{ if } r > 0 \end{cases} , \tag{1}$$

where $a > 0$ and $b < 0$ are parameters controlling the slopes. This function is sometimes also referred to as lin-lin loss function [53]. When the loss function is normalised by dividing with the value $a - b$, it can
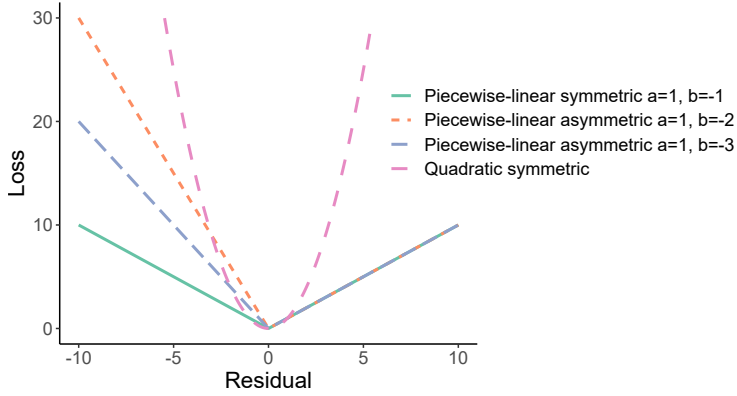
Figure 1: Illustration of loss functions.

be rewritten as a function of one parameter $\theta = a/(a - b)$. Typically, such reformulation is used in the context of the quantile regression [54]. Apart from the simplicity, the piecewise-linear function facilitates the interpretability of obtained results (see Section 3.4.3). Moreover, compared to the quadratic function, the piecewise-linear function applies relatively higher penalty to small residuals and smaller penalty to higher residuals [55]. In the context of the smart charging, we can expect that if the prediction loss exceeds a certain limit, it does not influence the performance of a smart charging scheme anymore. Also for this reason, the piecewise-linear function can be seen as a suitable modelling option.

2.2 Prediction methods

We consider training data with P features and N observations. By the symbol y_i, we denote i-th observation of the target variable (i.e., the duration of the i-th charging session in the training set) and x_{ij} denotes i-th observation of the j-th feature. Considering a single unspecific observation, all feature values form a vector $\boldsymbol{x}$. For the k-th observation of all features in the training set, we use the symbol $\boldsymbol{x}_k$.

2.2.1 Quantile regression with L_1 and L_2 penalties

Quantile regression (QR) is an extension of the linear regression [56], where the quadratic loss function is replaced by the linear asymmetric loss function (1). Here, we apply L_1 and L_2 regularisation, whose role is to shrink or select the regression coefficients [57, 58]. The estimate of regression coefficients is obtained by solving the problem

$$\underset{\beta_0, \beta}{\text{minimise}} \left\{ \frac{1}{2N} \sum_{i=1}^{N} \rho\left(y_i - \beta_0 - \sum_{j=1}^{P} x_{ij}\beta_j\right) + \lambda\left(\frac{1-\alpha}{2} \sum_{j=1}^{P} \beta_j^2 + \alpha \sum_{j=1}^{P} |\beta_j|\right) \right\}, \tag{2}$$

where β_0 is the intercept and β_j is the regression coefficient associated with j-th feature. Here $\lambda \geq 0$ is the hyperparameter controlling the strength of the regularisation, and $\alpha \in \langle 0, 1 \rangle$ sets the trade-off between L_1 and L_2 penalties.

2.2.2 Gradient Boosted Regression Trees

The gradient tree-boosting algorithm (GBRT) recursively fits a regression tree to residuals derived from predictions of the previously created sequence of regression trees [59]. Computation of residuals requires evaluation of the gradient vector, where the loss function takes the form (1). The prediction of the target variable $f^{(i)}(\boldsymbol{x})$ at the iteration i (each iteration is associated with a decision tree) for a vector of feature values $\boldsymbol{x}$ is given by the equation:

$$f^{(i)}(\boldsymbol{x}) = f^{(i-1)}(\boldsymbol{x}) + \nu \sum_{j=1}^{J^{(i)}} \omega_j^{(i)} \mathbb{1}(\boldsymbol{x} \in R_j^{(i)}), \tag{3}$$

where $J^{(i)}$ is the number of leaf nodes of the i-th regression tree, $R_j^{(i)}$ is the domain of the j-th leaf node, ν is the shrinkage parameter and $\omega_j^{(i)}$ is a real value associated with the j-th leaf node during the training process. The function $1(\cdot)$ takes the value 1 if the expression in the brackets is true and 0 otherwise.

2.2.3 Neural networks

Neural network (NN) is a powerful nonlinear regression technique [60]. Response vector is modelled by the set of M hidden layers, where the i-th layer contains $M^{(i)}$ neurons that return linear combinations of neuron outputs from the previous layer, transformed by a nonlinear activation function $s(\cdot)$. The output of the k-th neuron at the layer $i + 1$ is given by the equation

$$g_k^{(i+1)}(g^{(i)}) = s\left(\gamma_{0k}^{(i)} + \sum_{j=1}^{M^{(i)}} \gamma_{jk}^{(i)} g_j^{(i)}\right), \tag{4}$$

where $\gamma_{jk}^{(i)}$ is the parameter representing the weight of the link connecting j-th neuron from the i-th layer with the k-th neuron from $i + 1$-th layer, and $\gamma_{0k}^{(i)}$ is a parameter representing the constant term in the linear combination. For the initial layer ($i = 0$), the input is the vector of feature values $\boldsymbol{x}$, thus $g^{(0)} = \boldsymbol{x}$. The prediction of the target variable $g(\boldsymbol{x})$ returned by a neural network with M layers can be described as a nested sequence of values that propagate through layers, i.e.,

$$g(\boldsymbol{x}) = g^{(M)}\Big(g^{(M-1)}\big(\ldots, g^{(0)}(\boldsymbol{x}), \ldots, \big)\Big). \tag{5}$$

To set the parameter values $\gamma_{jk}^{(i)}$ and $\gamma_{0k}^{(i)}$, we minimise the function

$$\mathcal{L} = \sum_{i=1}^{P} \rho\big(y_i - g(\boldsymbol{x}_i)\big) \tag{6}$$

representing a model loss involving asymmetric loss function.

2.2.4 Naive methods

To assess the effects resulting from using advanced prediction methods, we apply three naive prediction methods. The first method returns as an estimate the mean of all previous charging session durations (MEAN). The second method provides as an estimate the median of all previous charging session durations (MEDIAN). Finally, the last naive method returns the 0.2-quantile of all previous charging session durations (0.2-QUANTILE).

2.3 Target variable and features

We consider the connection duration as the target variable, since it is the critical parameter for smart charging schemes. Considering the previous studies [31, 39, 41, 37, 36, 61] and the results of preliminary numerical experiments, we compiled from the charging sessions in the EVnetNL dataset the following set of features that potentially impact the target variable:

1. A feature specific to an EV driver and charging station pair characterising the charging process:

   - the maximum power an EV driver can charge at a given charging station (estimated as the minimum of the charging station's maximum power and the EV's maximum power) [1 feature].

2. Features capturing the long term charging history calculated from all the preceding charging sessions:

   - the median of the connection/charging duration for the station/EV driver associated with the charging session [4 features],
   - the mean start hour of a charging session initiated at the charging station/by the EV driver associated with the charging session (trigonometric transformations were applied to encode each time information with two features) [4 features].

3. Features characterising the most recent charging behaviour:

- the mean connection duration/the number of recent charging sessions in the previous one/seven days taken at the charging station/by the EV driver [8 features],
- the mean connection duration of the last one/ten charging sessions at the charging station associated with the predicted charging session [2 features],
- the mean connection duration of the last one/five charging sessions taken by the EV driver associated with the predicted charging session [2 features].

4. Features describing the initial time of the charging session:

- the start hour of the charging session encoded categorically. To decrease the number of features, we merged two consecutive hours into one category, e.g., the time between 2:00 and 3:59 appears as a category corresponding to 2:00 [1 feature described by 12 categories],
- the binary variable indicating whether the day when the charging session was initiated is a weekday [1 feature].

In groups 2, 3 and 4, the values are calculated considering a specific set of previously completed charging sessions for each feature. The daytime information requires cyclical encoding in order to maintain uniform distances among all values, e.g., the distance between 11:00 p.m. and 1:00 a.m. should numerically be equal to the distance between 5:00 a.m and 7:00 a.m. Therefore, we apply trigonometric transformations [36], resulting in two features for each daytime value. Altogether, we characterise a charging session with 23 features. We discarded the initial charging sessions after calculating the variable values as there is no history for such sessions. When required by the prediction method, we applied one-hot encoding [60] to categorical features.

2.4 Comparison of prediction methods

The performance of the prediction methods is quantified using the loss function given by Eq. 1. We apply the mean absolute error (MAE):

$$\text{MAE} = \sum_{i=1}^{T} \frac{\rho(r_i)}{T}, \tag{7}$$

where r_i is the residual obtained on the i-th observation. Further, we apply the median absolute deviation (MAD):

$$\text{MAD} = \text{Median}(|\rho(r_1) - \text{MED}|, \ldots, |\rho(r_T) - \text{MED}|), \tag{8}$$

where $\text{MED} = \text{Median}(\rho(r_1), \ldots, \rho(r_T))$. To facilitate the comparability with studies that apply the quadratic loss function, we also report the value of the Root Mean Square Error (RMSE) :

$$\text{RMSE} = \sqrt{\frac{\sum_{i=1}^{T} \rho(r_i)^2}{T}}. \tag{9}$$

When contrasting the prediction performance with other studies, we evaluate the symmetric mean absolute percentage error (SMAPE):

$$\text{SMAPE} = \frac{100\%}{n} \sum_{i=1}^{n} \frac{|r_i|}{(|y_i| + |y_i + r_i|)/2}. \tag{10}$$

The values of all metrics are calculated using the test set.
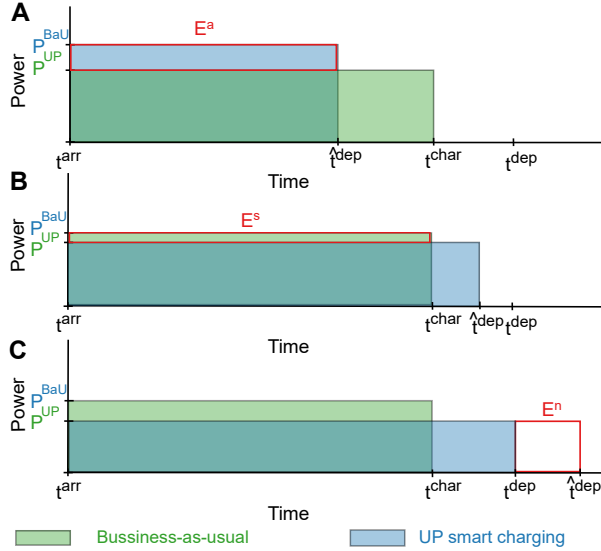
Figure 2: Comparison of the UP and the BaU charging schemes. The underestimation of the connection duration: **A** causes an unnecessary increase in the charging power, **B** enables a reduction of the charging power. **C** The overestimation of the connection duration leads to lower charging power at the expense of not charged energy.

2.5 Smart charging schemes

According to [8, p. 106] charging can be optimised along three dimensions: the time (by postponing the charging), the speed (by increasing or decreasing the charging power), and the charging direction (by switching between charging and discharging of an electric vehicle, i.e., vehicle to grid approach). The number of smart charging schemes proposed in the literature [10, 11] is overwhelming and each of them is putting a stress on different aspects. Here, we consider one baseline scheme that represents business-as-usual case of uncontrolled charging and two archetypal smart charging schemes optimising the charging time and speed. The schemes are introduced together with main indicators enabling the quantification of the consequences of under- and over-estimation of the charging duration. We intentionally applied only archetypal examples of smart charging schemes capturing the main characteristics to ensure the higher generalisability of our conclusions.

2.5.1 Business-as-usual charging

As a baseline, we consider a business-as-usual (BaU) charging scheme, where no smart charging scheme is employed [62]. The charging is initiated at the time t^{arr} when the driver plugs in the vehicle to the station. Charging continues either until the vehicle is fully charged or the driver unplugs it, denoted as the time t^{char}, and it is performed with (nearly) uniform power P^{BaU} (see Figure 3B). In computational experiments, all the sessions' parameters are taken from the EVnetNL dataset.

2.5.2 Uniform power smart charging

The uniform power (UP) smart charging scheme is a representative of smart charging schemes that modulate charging power to meet the needs of EV drivers and power grids. Such schemes are in the literature also referred to as controlled charging [63]. The scheme sets the charging power to a session-dependent constant. To distribute the load over time, the charging power equals to the minimum possible value, while maintaining a chance that an EV gets all demanded energy. Thus, the charging power is given by the ratio between the demanded energy and the estimated connection duration.

The under- and over-estimation of the connection duration directly affect the charging process. In Figure 2A, we illustrate the situation when the underestimation of the connection duration (i.e., $\hat{t}^{dep} < t^{dep}$) leads to higher charging power P^{UP} than would be the power P^{BaU} applied by the BaU charging strategy. This effect can be quantified by the energy E^a, that would be charged at the power corresponding to $P^{UP} - P^{bau}$. On the contrary, an accurate estimation of the connection duration (i.e., if $\hat{t}^{dep} \approx t^{dep}$
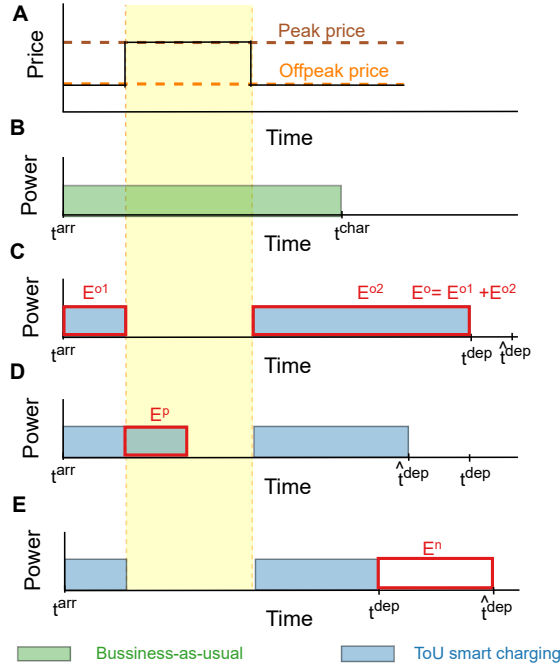
Figure 3: Comparison of the BaU and the ToU smart charging schemes. **A** Price signal. **B** Business-as-usual charging scheme. **C** time-of-use charging scheme, where the high price period is fully avoided. **D** time-of-use charging scheme, where the high price period is only partially avoided. **E** time-of-use charging scheme, where the high price period is entirely avoided, but less energy than by the business-as-usual scheme is provided to the vehicle due to the overestimation of the connection duration.

as shown in Figure 2B) leads to the lower value of the charging power P^{UP} than is the power P^{BaU}. Such effect can be quantified by the energy E^s that would be charged at the power $P^{bau} - P^{UP}$. A more significant overestimation of the connection duration lowers the charging power, but it also results in the energy, E^n, which is demanded but not charged (see Figure 2C).

2.5.3 Time-of-use smart charging

The ToU smart charging scheme is based on the price signal that varies over the predetermined price periods of the day in response to the power grid state [63, 14]. The price tends to grow together with the load. For simplicity, we consider only two price levels: peak price and off-peak price (see Figure 3A). EV is assumed to be charged at maximum possible power. The ToU scheme requires the (estimated) connection duration and the price periods as an input. Considering these inputs, the charging process is preferably arranged in the off-peak price period and as early as possible. Hence, the charging takes place in the peak price period only if the EV cannot be fully charged in the off-peak price period.

Consequently, over- and under-estimation of the connection duration may have different effects. A reasonably precise estimate of the connection duration (i.e., if the estimated time of departure $\hat{t}^{dep}$ approximately equals to the true departure time t^{dep}) may allow avoiding peak price periods completely, without reducing the energy charged (see Figure 3C). Thus, the energy charged in the off-peak price periods, E^o, equals the energy charged by the BaU scheme (shown in Figure 3B). As illustrated in Figure 3D, the underestimation of the connection duration (i.e., if $\hat{t}^{dep} < t^{dep}$) can lead to charging in the peak price period, even though it is not necessary. Consequently, the energy charged in the peak price period, E^p, is non-zero. The overestimation of the connection duration, may lead to the charging schedule that avoids the peak price period. However, if the vehicle is unplugged earlier than estimated (i.e., if $\hat{t}^{dep} > t^{dep}$), it is not charged to the same extent as in the case of the BaU scheme. This effect can be quantified by the amount of energy that has not been charged, E^n (see Figure 3E).

2.6 The assessment of consequences of under- and over-estimation of the connection duration

We utilise the concept of a cost function to evaluate the consequences of under- and over-estimation of the connection duration. We combine individual criteria by using weights that are considered as parameters. To evaluate the effects of the under- and over-estimation of the connection duration on the UP smart charging scheme, we consider T individual charging sessions and the following quantities as individual criteria:

- $E^l = \sum_{i=1}^{T} E_i^a - \sum_{i=1}^{T} E_i^s$ - the total energy that is charged at a higher (if positive) or lower (if negative) power than the charging power applied by the BaU scheme,

- $E^n = \sum_{i=1}^{T} E_i^n$ - not charged energy due to an earlier departure than estimated.

The cost function to be assessed is:

$$w^l E^l + w^n E^n, \tag{11}$$

where w^l and w^n are non-negative weights. Similarly, for the ToU charging scheme, we consider the following individual criteria:

- $E^o = \sum_{i=1}^{T} E_i^o$ - total energy charged in the off-peak price period in all T individual charging sessions,

- $E^p = \sum_{i=1}^{T} E_i^p$ - total energy charged in the peak price period in all T individual charging sessions,

- $E^n = \sum_{i=1}^{T} E_i^n$ - total energy that could not be charged in all T individual charging sessions due to the lack of the charging time resulting from the connection duration over-estimation.

Thus, the cost function to be assessed is:

$$w^o E^o + w^p E^p + w^n E^n, \tag{12}$$

where w^o, w^p and w^n are non-negative weights. The value of $E^o + E^p + E^n$ is independent of the loss function parameters a and b. Consequently, we evaluate the ToU scheme in the parameter space given by the differences $w^p - w^o$ and $w^n - w^o$.

2.7 Data processing and construction of models

From the EVnetNL dataset, we chose only the most recent charging sessions that started on January 1st, 2016 or later and ended at latest on June 30th, 2018. As the data collection has been running for several years, the EVnetNL dataset is of very good quality. We eliminated a few sessions with zero charging duration where a non-zero energy was charged. We capped connection duration and charging duration to 24 hours since in some cases they span over a long period (e.g. several weeks).

The data was partitioned into four non-overlapping subsets. The warm-up subset was used to compute the values of history-dependent features. For such subset, we selected all sessions that started in 2016. The training subset was used to train prediction models. Such subset covered the period between January 1st, 2017 and October 31st, 2017. The validation subset was used to tune the values of hyperparameters. Such subset included charging sessions taking place between November 1st, 2017 and February 28th, 2018. The remainder of the data constituted the test subset, used to evaluate prediction models. To ensure a minimum level of historic information, we considered only sessions associated with a charging station and an EV driver, each having at least ten sessions. In addition, at least one of the sessions associated with a charging station or an EV driver must be included in each of the training, validation and test subsets. Finally, the data entering the analysis contains 999 charging stations, more than 4k drivers and 189k charging sessions. The data was cleaned, and features were extracted in R using *tidyverse* and *lubridate* packages. To prepare the data for the neural networks, we used the *sklearn* Python library.

2.8 Parameter settings

The R package *hqreg* was chosen to implement the QR method. We employed the grid search to find the best values of hyperparameters. The hyperparameter α was taken from the interval 0 to 1 in steps of 0.01. The hyperparameter λ was set to 10^i with i from -5 to 1 in steps of 0.01.

For computationally expensive methods, i.e., GBRT and NNs, we utilised a random hyperparameter search [64]. For each hyperparameter, a vector of n realisations was randomly generated. Vectors were then merged to form a matrix with n rows, where each row contained a realisation of all hyperparameters. For both, GBRT and NNs, we generated $n = 200$ samples of hyperparameter values. The best combination of hyperparameters was chosen by evaluating the models on the validation subset.

To implement the GBRT method, the R package *gbm* was used. The hyperparameter ν was taken from the uniform distribution $\mathcal{U}_{[0.01, 0.3]}$ and tree depth from $\mathcal{U}_{\{5,15\}}$. The maximum number of iterations (i.e., the total number of trees to fit) was fixed to 500. The iteration with lowest validation error was chosen for predictions. The Python libraries *keras* and *tensorflow* were used to implement the NN method. The RELU function was selected as the activation function. We applied $M = 2$ deep layers with $64, 128, 256$ neurons in each layer. For each layer, we selected the values of dropout from $\mathcal{U}_{[0,0.3]}$. We applied the ADAM optimiser, with the learning rate from $\mathcal{U}_{[0.0001, 0.001]}$. We executed 200 training epochs, while the learning rate was scheduled to decay exponentially after the first 100 epochs. The epoch with lowest validation error was chosen for predictions. With NN, we tested L_1 and L_2 regularizers, but none of them improved the results. The loss function parameter b ranges from -8 to -1 in steps of 1, for every method. For the UP scheme we set the minimum charging power to $0.2\ kW$ to prevent charging with unreasonably small power.

3 Results

We start this section by introducing and analysing the EVnetNL dataset, to verify its suitability for smart charging. Afterwards we compare prediction methods and evaluate the impact of the loss function asymmetry on the performance of smart charging schemes.

3.1 EVnetNL dataset

Computational experiments presented in this study are based on the EVnetNL dataset that has been provided to us for research purposes by the ElaadNL, a Dutch knowledge and innovation centre in the field of smart charging and the charging infrastructure [65]. The dataset is composed of two tables, "Transactions" and "Meterreadings". The table "Transactions" describes charging sessions by the charging point and connector identifiers, latitude and longitude, initial and terminal times, initial and terminal states of the meter, and identifiers of the driver radio-frequency identification (RFID) cards used to initiate and terminate charging sessions. Records stored in the table "Meterreadings", describe the energy consumption with the frequency of 15 minutes. The data span from 01/2012 to 06/2018, cover 1700 public and semi-public charging stations, about 82k drivers, more than 1.8M charging sessions, and more than 52M meter readings. In the initial years the charging network features a small number of charging stations followed by the rapid growth. The numbers have been stabilised shortly before 2015 [61]. The maximum power ranges from 3 to 12 kW [61], i.e., charging stations included in the dataset correspond to the slow-charging. Since 2017 are all charging stations smart charging ready, but except a few smart charging trials, in the time period covered by the used data there was no smart charging scheme in place. Thus, the charging starts immediately as the EV is plugged into a charging station and continues at approximately constant power either until the battery is fully charged or until the EV is unplugged.

3.2 Data analysis

The purpose of the data analyses is twofold. First, we focus on temporal characteristics of charging sessions that are later used in predictions. Second, we assess the applicability of the smart charging in the EVnetNL charging network. In Figure 4, we present the temporal characteristics of the EVnetNL charging sessions. The shape of the density function of the connection duration strongly depends on the start hour of charging sessions (see Figure 4A). Towards the evening hours, the density function becomes bi-modal. This can be explained by a small fraction of EV drivers that unplug vehicles during the night. Panel B of Figure 4 shows that the pattern formed by the start hour of sessions is different at working days and at weekends. On working days, the number of initialised sessions features two peaks, one in the morning and one in the afternoon, while during the weekends, it grows in the morning, peaks around noon, and decreases afterwards. In Panels C-F of Figure 4, we show the empirical distributions of the mean of connection duration and charging duration for charging stations and EV drivers together with
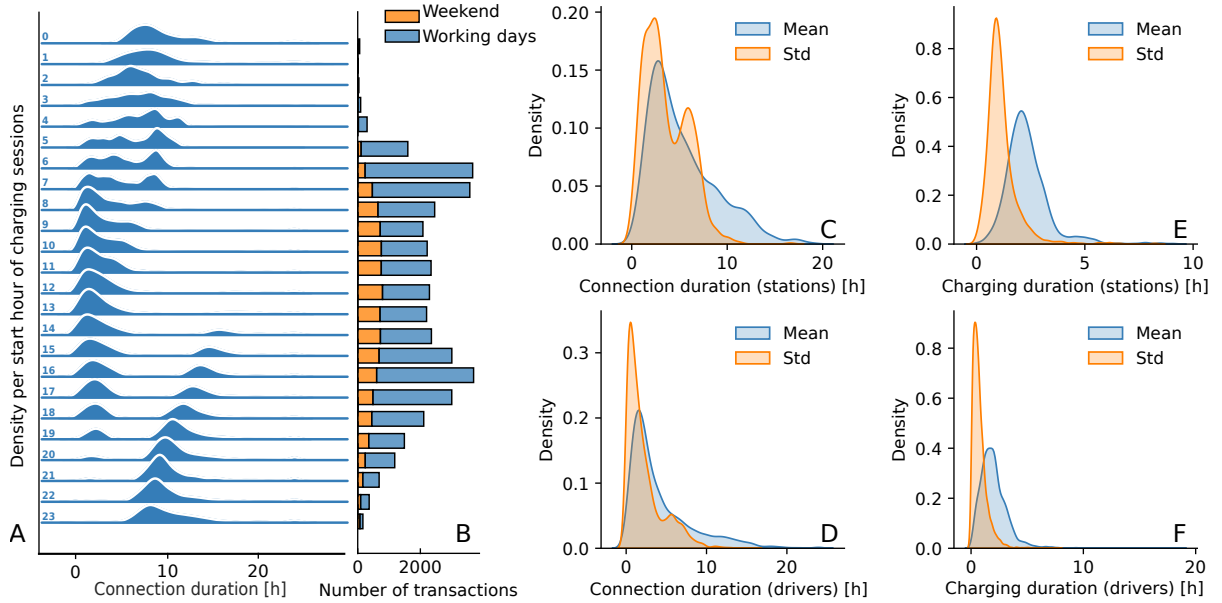
Figure 4: Temporal characteristics of charging sessions. **A** Probability densities of connection duration for different start hours of sessions. **B** The number of charging sessions by start hour (the numbers of sessions with a start hour on weekends and working days are stacked). **C** and **E** Probability densities of the mean connection duration and mean charging duration together with standard deviations (the mean values and standard deviations are calculated for individual charging stations). **D** and **F** Probability densities of the mean connection duration and mean charging duration together with the standard deviations (the mean values and standard deviations are calculated for individual drivers).

distributions of the corresponding standard deviations (Std). The distribution of the mean connection duration is relatively broad and bi-modal for both, charging stations and EV drivers. Likewise, the mean charging duration shows a very similar distribution across stations and drivers. Hence, in this respect, stations and drivers behave similarly; however, the broad range of values and bi-modality confirm a complex pattern of the connection duration, making it challenging to predict. At the same time, our analysis reveals some potentially relevant features such as hour of the day, day of the week, and type of the EV driver and charging station.

To assess the relevance of applying a smart charging scheme in the EVnetNL network, we visualise in Figure 5 the number of active charging sessions as a function of the hour of the day at working days and weekends. Over the weekends, the number of active charging sessions is relatively stable; however, during working days, it fluctuates significantly, peaking around the noon and during the night. Interestingly, the valleys are observed at times when the consumption of electricity reaches the maxima (see Figure 5B), indicating the potential to optimise the charging in a way that would reduce the energy consumption peaks. Comparison of the connection duration with charging duration (in Figure 4) already indicates that charging takes only a fraction of the connection duration, raising a the possibility to apply a smart charging scheme. To analyse it in more detail, in Figure 5 we show how the idle ratio, i.e., the ratio between the time when a vehicle is connected to a station, but it is not charged and the overall connection duration, as a function of the hour of the day. The idle ratio has the opposite trend as the consumed energy confirming the high potential for applying a smart charging scheme.

By examining the charging patterns in Figure 5(B), we identified two peak periods with a large energy consumption. The morning peak lasts from 8:00 till 11:00, and the afternoon peak from 17:00 to 21:00. In numerical experiments, we set the peak price periods in the same way. The remainder we defined as the off-peak price period.

3.3 Comparison of prediction methods

The values of performance indicators, described in Section 2.4, are presented in Table 1. To keep the presentation concise, only the results for $b = -1$ and $b = -4$ are displayed. For other values, please refer
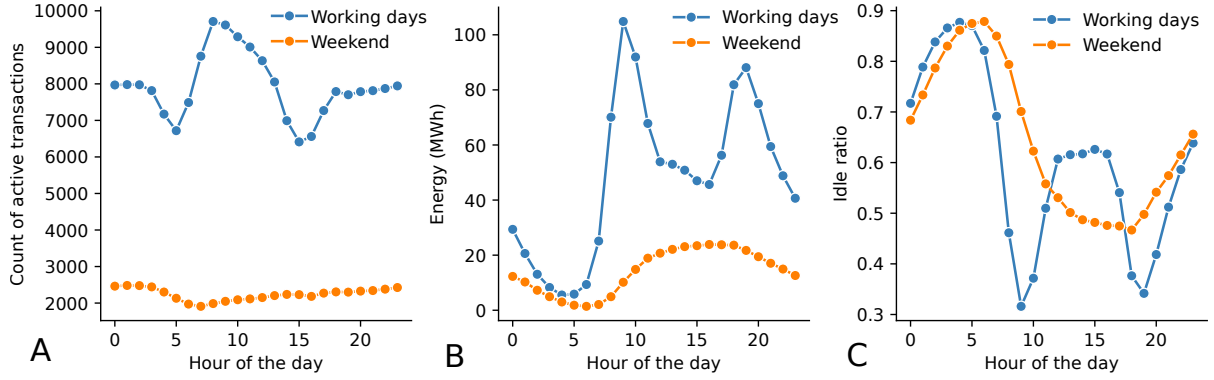
Figure 5: Temporal analysis of charging sessions. **A** Number of active charging sessions as a function of the time of the day. **B** Consumed energy as a function of the time of the day. **C** Idle time ratio as a function of the time of the day.

Prediction method	MAE ($a = 1$, $b = -1$)	MAD ($a = 1$, $b = -1$)	MAE ($a = 1$, $b = -4$)	MAD ($a = 1$, $b = -4$)	RMSE ($a = 1$, $b = -1$)	RMSE ($a = 1$, $b = -4$)
MEAN	4.81	4.44	12.31	12.18	5.83	14.46
MEDIAN	4.45	3.09	7.98	7.76	6.19	9.39
0.2-QUANTILE	5.06	2.46	5.52	3.65	7.52	7.66
QR ($a = 1$, $b = -1$)	2.76	1.52	6.55	3.21	4.23	11.28
QR ($a = 1$, $b = -4$)	3.82	2.00	4.57	2.87	5.85	6.58
GBRT ($a = 1$, $b = -1$)	2.43	1.20	5.54	2.56	**4.07**	10.09
GBRT ($a = 1$, $b = -4$)	3.16	1.51	3.99	2.12	5.23	**6.52**
NN ($a = 1$, $b = -1$)	**2.38**	**1.13**	5.54	2.47	4.10	10.61
NN ($a = 1$, $b = -4$)	3.05	1.39	**3.90**	**1.91**	5.19	6.78

Table 1: The performance of prediction methods on the test subset. All values are reported in the units of hours.

to the Table S1 Supplementary Information file. The performance of naive models (MEAN, MEDIAN and 0.2-QUANTILE) is significantly outperformed by the advanced models (QR, GBRT and NN), justifying their construction. As expected, the performance indicators with the same asymmetry as in the loss function give the most favourable values. The difference between GBRT and NN is relatively small, but the NN model is systematically better. Therefore, we consider the NN model in further analyses. The comparison of the prediction performance with studies in the literature [37, 33] is not straightforward. The main limitation is in different datasets used by other studies. The datasets describe a different type of charging system (e.g. slow or fast charging), different environment (e.g. residential or non-residential) or different type of charging (e.g. private or public), etc. These differences influence the distribution of the connection duration while affecting the achievable accuracy of predictions. Thus, instead of comparing the absolute accuracy of predictions, in Table 2 we evaluate the improvement of predictions provided by the best performing model with respect to the prediction accuracy achieved by a naive model. In [37], the best performance was achieved by the XGBoost algorithm, MAE = 1.36 hours, while the naive model MEDIAN reached MAE = 1.73 hours. Thus the XGBoost lowers the MAE by 27.20 %. On the EVnetNL data, the NN method, with $a = 1$ and $b = -1$, lowers the MAE by 84.65 %. Similarly, in [33] predictions of the connection duration are made on two datasets: JPL and Caltech. The best performance, evaluated by the SMAPE, was achieved by the individual-level Gaussian mixture model. On the JPL (Caltech) dataset, the SMAPE was lowered by 29.78 % (28.97 %) with respect to the naive model MEAN. The NN model, with $a = 1$ and $b = -1$ achieved an improvement of SMAPE by 81.15 %. In this respect, the advanced prediction models proposed in this study significantly outperform models presented in [37, 33].

Reference - Dataset	MAE (best method) [hours]	MAE (ME-DIAN) [hours]	MAE improvement [%]	SMAPE (best method) [%]	SMAPE (MEAN) [%]	SMAPE improvement [%]
This paper - EVnetNL	2.41	4.45	**84.65**	22.71	41.14	**81.15**
Ref. [37] - German dataset	1.36	1.73	27.20	-	-	-
Ref. [33] - JPL dataset	-	-	-	12.25	15.9	29.78
Ref. [33] - Caltech dataset	-	-	-	15.85	20.44	28.94

Table 2: Comparison of the prediction performance of the NN model (the best model in this paper) with the best models presented in other studies. The comparison is made by evaluating the percentual improvement of a given performance indicator with respect to a naive model.

Method	E^n [MWh]	E^a [MWh]	E^s [MWh]
BaU	0.0	0.0	0.0
Oracle	0.0	0.0	129.2
NN (a = 1, b = -1)	42.0	9.6	66.8
NN (a = 1, b = -2)	25.0	17.6	70.4
NN (a = 1, b = -3)	17.8	24.3	67.0
NN (a = 1, b = -4)	13.1	30.1	61.9
NN (a = 1, b = -5)	9.7	35.8	56.7
NN (a = 1, b = -6)	9.1	37.1	54.6
NN (a = 1, b = -7)	7.4	41.4	50.2
NN (a = 1, b = -8)	6.2	45.4	45.5

Table 3: The performance of the UP smart charging scheme assessed by three individual criteria (E^n - demanded but not delivered energy, E^a - energy charged at high power, E^s - energy charged at low power). The performance of the NN model is compared with two benchmarks: BaU, where no smart charging is applied, and the Oracle method, where the UP smart charging is applied with actual values of the connection duration taken from the EVnetNL dataset.

3.4 Impact of cost-sensitive predictions on smart charging schemes

To evaluate the impact of cost-sensitive predictions on the performance of smart charging schemes, we estimated the connection duration with the NN method for charging sessions in the test subset and emulate the control of the charging process by the UP and ToU smart charging schemes. We quantified the performance of smart charging schemes by the criteria described in Section 2.6. To contrast the results with some benchmarks, we included the BaU scheme, where no smart charging is applied. Furthermore, we combined both smart charging schemes with actual values of the connection duration, denoted as the Oracle method.

3.4.1 Uniform power smart charging scheme

Table 3 shows the obtained values of the criteria introduced in Section 2.5.2 for the considered prediction methods. The BaU scheme is used as a reference case; hence the values of all criteria are zero. The Oracle method indicates the full potential, how the charging could be improved with errorless predictions. With the Oracle method, the energy $E^s = 129.2$ MWh was charged on a lower power than the BaU. As expected, by decreasing the value of b (increasing the asymmetry of the loss function), the value of E^n decreases. This is compensated by the growing amount of the energy charged at higher power (E^a) and by the decreasing amount of the energy charged at lower power (E^s). Interestingly, when analysing the relative changes in Table 3, we see that the demanded but not charged energy E^n first decreases very fast, and from $b = -5$ onward, decreases become minor. Likewise, first we observe fast growth (decrease) of the E^a (E^s) that becomes roughly constant from $b = -5$ onward.

To get a better idea about the real-world effects of aggregated results presented in Table 3, we translate them to one charging session. For the loss function with $b = -1$, the average value of E^n is 1.02 kWh per session. Assuming the average consumption of 15 kWh per 100km, the value of 1.02 kWh corresponds

Method	E^n [MWh]	E^p [MWh]	E^o [MWh]
BaU	0.0	150.2	194.5
Oracle	0.0	66.0	278.6
NN (a = 1, b = -1)	22.4	57.8	264.4
NN (a = 1, b = -2)	13.4	76.9	254.4
NN (a = 1, b = -3)	9.5	88.8	246.3
NN (a = 1, b = -4)	7.1	98.4	239.2
NN (a = 1, b = -5)	5.2	106.9	232.6
NN (a = 1, b = -6)	4.7	110.0	230.0
NN (a = 1, b = -7)	3.7	115.7	225.2
NN (a = 1, b = -8)	2.9	120.7	221.0

Table 4: The performance of the ToU charging scheme assessed by three individual criteria (E^n - demanded but not delivered energy, E^p - energy charged at peak price, E^o - energy charged at off-peak price). The performance of the NN model is compared with two benchmarks: BaU, where no smart charging is applied, and Oracle, where ToU smart charging is applied with actual values of the connection duration taken from the EVnetNL dataset. Each row sums up to 344.6 MWh, i.e., the total energy demanded.

to 6.82 km of driving distance. With $b = -8$, E^n is only 0.22 kWh per session, i.e., 1.48 km of driving distance. This improvement may be sufficient to affect the driving range, considering the average energy charged per session of 8.4 kWh (56 km driving range).

3.4.2 Time-of-use smart charging scheme

In Table 4 we show the values of the evaluation criteria attained by the ToU smart charging scheme. Without smart charging, 150.2 MWh are charged at the peak price and 194.5 MWh at the off-peak price. The ToU smart charging scheme, with perfect predictions, resulted in 66.0 MWh charged at the peak price and 278.6 MWh at the off-peak price. In both cases, the amount of demanded but not delivered energy, E^n was 0 MWh. For the symmetric loss function E^n was 22.4 MWh. By making $b = -2$, the E_n decreases by 9 MWh on the expense of increasing the energy charged at the peak price, E^p, by 19.1 MWh and reducing by 10 MWh the energy charged at the off-peak price, E^o. By increasing the asymmetry of the loss function, i.e., by decreasing the value of the b parameter, the energy E^n and the energy E^o decrease while the energy E^p increases. Again, when assessing the changes in the criteria, first all quantities change rapidly. Approximately from $b = -5$ the changes become relatively small. The relative changes in individual criteria can help select a suitable level of the asymmetry parameter b.

If converting the numbers in Table 4 to one charging session, for $b = -1$ we get $E^n = 0.54$ kWh per session, corresponding to 3.64 km of driving distance. For $b = -8$, we obtain $E^n = 0.07$ kWh per session or 0.47 km of driving distance. Hence, using the asymmetric loss function strongly eliminates the impact of E^n on the driving range. These numbers assume the energy consumption of 15 kWh per 100km.

3.4.3 Summary of results

To analyse cost functions (11) and (12), we draw in Figure 6 diagrams indicating by colours the charging scheme with the minimum cost for different combinations of weights. Panel 6A shows that the asymmetric loss functions outperform the symmetric loss function in large part of the space formed by weights. The BaU scheme is a reference case for evaluations; hence it cannot be compared with other schemes in panel 6A. In panel 6B, there is an area where the BaU scheme leads to the minimum cost. Again, the panel illustrates that the asymmetric loss functions dominate over symmetric in a certain region of weights. In both panels we show the otherwise invisible borderlines where pairs of charging schemes reach the same costs. The cone in panel 6B, bounded by the pink borderline between $b = -1$ and BaU and the purple borderline between $b = -8$ and BaU, represents the area where the ToU smart charging dominates over the BaU scheme thanks to asymmetric loss functions. Thus, asymmetric loss functions enlarge the applicability of the ToU smart charging scheme and decrease the total costs compared to the symmetric loss function.
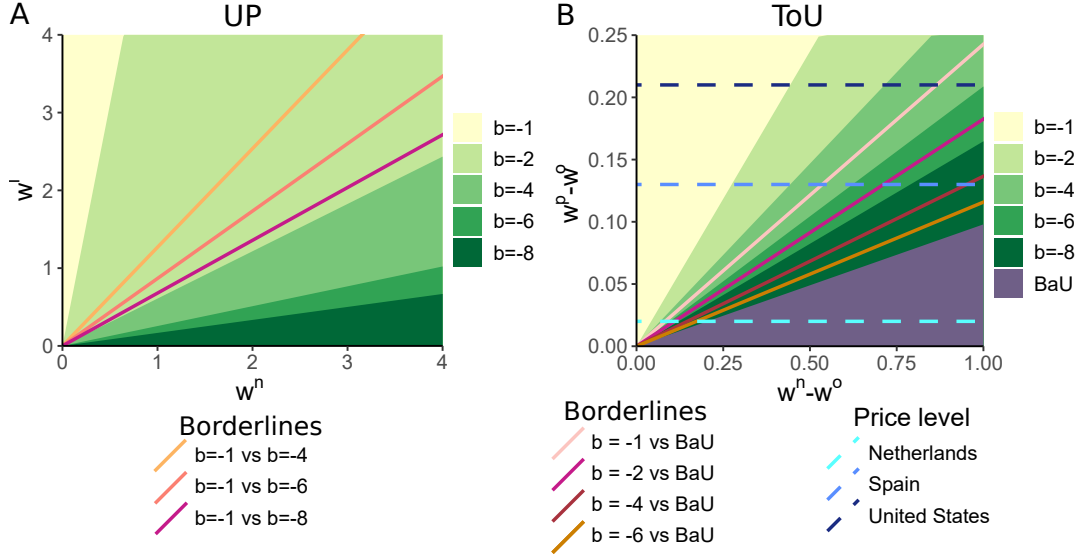
Figure 6: Diagram indicating by colours the areas of the weight space where a charging scheme (given by the value of the parameter b or the BaU scheme) results in the minimum value of the cost function. **A** The UP smart charging schemes. The solid lines are the borderlines where the cost functions obtained by asymmetric and symmetric loss functions take the same values. **B** The ToU smart charging schemes. The solid lines are borderlines where the cost functions obtained by the asymmetric loss function and the BaU scheme take the same values. The dashed lines correspond to the real price difference $w^p - w^o$ in selected countries. The range on the x-axis is larger as w^n can be expected to take a larger value than w^p. To keep the diagrams readable, we used only the values of $a = 1$ and $b \in \{-1, -2, -4, -6, -8\}$.

In panel 6B, we indicate by the dashed lines the price levels (the difference between the peak and off-peak price) for three selected countries: the Netherlands, Spain and the United States. The smart charging scheme operated by Ibedrola in Spain provides a subscription plan with nightly (off-peak) and daily (peak) prices of $w^o = 0.03$ and $w^p = 0.24$ EUR/kWh, respectively [66]. As the second scheme, we selected the Dutch smart charging provider GreenFlux EV with $w^o = 0.35$ the off-peak and $w^p = 0.37$ EUR/kWh the peak prices [67]. The US company Xcel Energy provides ToU smart charging for the average peak price of $w^p = 0.19$ EUR/kWh and off-peak price of $w^o = 0.06$ EUR/kWh [68].

The horizontal lines in panel 6B can serve as a decision support tool. The first possibility is to analyse whether the implementation of the ToU scheme pays off in comparison to the BaU. For example, let us consider the price levels w^p and w^o in the Netherlands, where the EVnetNL dataset was recorded. The dashed line corresponding to $w^p - w^o$ is positioned relatively low. Consequently, the range $w^n - w^o$, where the ToU smart charging pays off is relatively small, even though it is doubled by the asymmetric loss functions. Hence, the relevance of the ToU smart charging is undermined. For the ToU to become a more attractive option, the price difference $w^p - w^o$ should be enlarged, for example as it is in the case of Spain or the United States. The second possibility is to determine the point where the system operates. In such a case, the colour of the area indicates how to set the parameters a and b of the loss function. Unfortunately, in general it is difficult to establish the price w^n. The exception is some specific situations, e.g. if the EV driver uses an alternative charging opportunity, e.g., fast charging, to charge the energy E^n. In such a case, the value w^n is given by the fast charging price.

The previous numerical experiments showed that lowering the value of b decreases the demanded but not delivered energy E^n. To investigate how is the E^n distributed over the charging sessions, we calculated the ratio E^n/E, where E is the overall demanded energy by the charging session. Figure 7 shows the cumulative distribution functions (CDFs) obtained from the ratio values calculated across all charging sessions. For the symmetric loss function, the ratio E^n/E starts around the value of 0.5 (0.82) in the case of the UP(ToU). By increasing the asymmetry of the loss function, the smallest values of the ratio grow and reach the values around 0.9 and 0.97, respectively. In panel 7B, the CDF transitions to the value 1 at $E^n/N = 1$. The corresponding step size indicates the proportion of sessions when EVs received no energy. This proportion decreases from 0.034 when $b = -1$ to 0.076 when $b = -8$, demonstrating
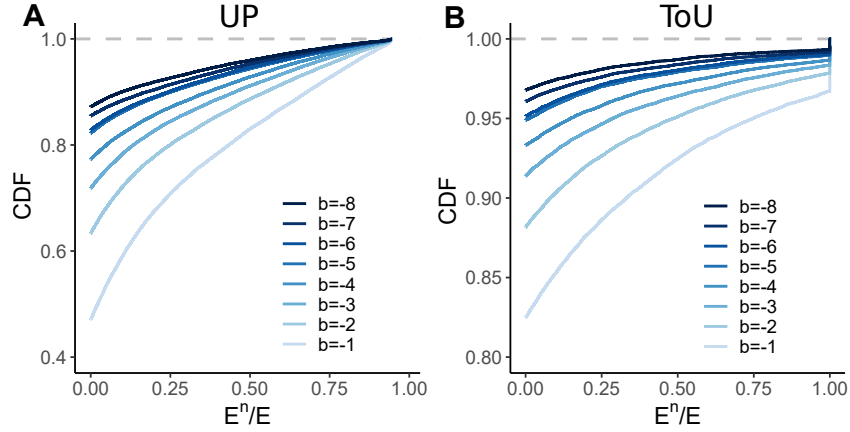
Figure 7: The cumulative distribution functions of the fraction of energy (E^n/E) that was demanded but not delivered due to the early departure. **A** The UP smart charging scheme. **B** The ToU smart charging scheme. The grey dashed line represents the CDF corresponding to Oracle predictions.

yet another benefit of asymmetric loss functions. Overall, the asymmetric loss function leads to a more homogeneous distribution of values E^n/E, making the charging of EVs fairer.

To check the robustness of predictions, we investigated whether prediction errors on consecutive series of charging sessions performed by individual EV drivers add up or eliminate each other. We selected EV drivers with at least 20 charging sessions for the analysis. The empirical probability of observing two consecutive sessions with overestimated connection duration of an EV decreases with the b parameter. For example, it is equal to 0.273 for $b = -1$ and 0.005 for $b = -4$. Thus, the asymmetric loss function decreases the likelihood of observing a series of overestimates. To see how prediction errors translate to charging schemes, we selected the demand threshold of 2 kWh (approximately 12 km of driving range). If the difference between requested and charged energy was below this threshold for a charging session, we considered the demand satisfied. For the ToU scheme, the probability of demand not being satisfied for two consecutive sessions was 0.013 ($b = -1$) and 0.002 ($b = -4$). For the uniform scheme this was 0.012 ($b = -1$) and 0.001 ($b = -4$). Hence, both schemes are robust as the probabilities of two consecutive charging sessions having unsatisfied demand are small. The asymmetric loss function increases the robustness.

4 Conclusions

We developed state-of-the-art prediction models for the connection duration with the asymmetric loss function and analysed the impact of asymmetries on the performance of charging schemes. Evaluating the performance of a smart charging scheme is a complex task as it is needed to assess several often contradicting perspectives. We proposed and applied an approach based on the cost function that combines several individual criteria. On two archetypal smart charging schemes, the uniform power and time-of-use, we observed that varying the degree of the asymmetry changes significantly the balance between performance criteria giving us a tool to harmonise a prediction model with a smart charging scheme. The asymmetric loss function brings valuable benefits:

- Predictions produced with asymmetric loss functions approximately double the area where the smart charging is profitable. For example, if we fix the price difference between peak and off-peak price to 0.09 EUR/kWh, it is more beneficial to use the time-of-use scheme than leave the system without smart charging if the costs difference between the energy demanded but not charged and the off-peak price is less than 0.41 EUR/kWh, if the used loss function is symmetric. With the asymmetric loss function ($b = -8$), it suffices if the costs difference is less than 1.03 EUR/kWh (see Figure 6). Consequently, the cost-sensitive predictions can extend the viability of business models implementing the smart charging schemes in practice.

- By penalising the negative residuals, asymmetric loss functions notably decrease the unmet charging demand at the expense of increased charging cost. For instance, in the case of the time-of-use scheme

19

the demanded but not supplied energy, E^n, is decreased by 40.2% when the symmetric loss function is replaced by the asymmetric with $b = -2$. The decrease happens at the expense of increasing by 33.0% the energy charged at the peak price and lowering by 3.9% the energy charged at the off-peak price. A higher level of satisfied demand lowers the chances that smart charging will disappoint EV drivers by leaving their vehicles with an insufficient state of charge.

- The demanded but not delivered energy may get not only smaller, but its distribution becomes more homogeneous (see Figure 7), making the smart charging fairer.

In summary, cost-sensitive predictions contribute to more efficient and viable smart charging and thus facilitate its adoption by EV drivers and infrastructure operators. The paper highlights the necessity to evaluate prediction models in the application context.

4.1 Limitations and Outlooks

The modelling choices imply the following limitations:

- We used archetypal charging schemes to evaluate the applicability of smart charging. The results could be changed, if charging schemes include more of technical details, although the main trends should be maintained.

- Similarly, the results might be data dependent to some degree. We used a single dataset, although it covers various EV charging behaviours, e.g., home charging, work charging, and opportunistic charging.

- The evaluation of smart charging schemes by the used cost function captures only the basic energy-related criteria and it does not consider more detailed requirements of infrastructure operators or EV drivers.

As a future work, how the used dataset could be utilised, we propose:

- To improve further the quality of predictions by implementing several prediction models instead of a single model to capture individual charging patterns of EV drivers. One approach could be to find clusters of similar EV drivers and train a model for each cluster.

- To update predictions in time as the charging session is unfolding, e.g., regularly or to optimise the frequency of updates.

- To develop customised prediction models for the EV induced load utilising online machine learning updating the model parameters in time.

Acknowledgements

References

[1] V. Masson-Delmotte, P. Zhai, A. Pirani, S. L. Connors, Péan, S. Berger, N. Caud, L. G. Y. Chen, M. I. Gomis, M. Huang, K. Leitzell, E. Lonnoy, J. Matthews, T. K. Maycock, T. Waterfield, O. Yelekçi, R. Yu, and B. Zhou, "IPCC, 2021: Summary for policymakers," tech. rep., 2021. Available as: `https://www.ipcc.ch/report/ar6/wg1/downloads/report/IPCC_AR6_WGI_SPM_final.pdf`.

[2] P. Moriarty and S. J. Wang, "Can electric vehicles deliver energy and carbon reductions?," *Energy Procedia*, vol. 105, pp. 2983–2988, 2017. 8th International Conference on Applied Energy, ICAE2016, 8-11 October 2016, Beijing, China.

[3] P. Wolfram, S. Weber, K. Gillingham, and E. G. Hertwich, "Pricing indirect emissions accelerates low—carbon transition of us light vehicle sector," *Nature Communications*, vol. 12, p. 7121, Dec 2021.

[4] H. Martin, R. Buffat, D. Bucher, J. Hamper, and M. Raubal, "Using rooftop photovoltaic generation to cover individual electric vehicle demand—a detailed case study," *Renewable and Sustainable Energy Reviews*, vol. 157, p. 111969, 2022.

[5] S. Powell, E. C. Kara, R. Sevlian, G. V. Cezar, S. Kiliccote, and R. Rajagopal, "Controlled workplace charging of electric vehicles: The impact of rate schedules on transformer aging," *Applied Energy*, vol. 276, p. 115352, 2020.

[6] GreenFlux, "Ev smart charging whitepaper," tech. rep., 2020. Available as: `https://www.greenflux.com/whitepaper/`.

[7] N. E. Agency, "Electric vehicle charging - definitions and explanation." `https://www.elaad.nl/uploads/files/Smart_Charging_Guide_EN_single_page.pdf`, 2019. Accessed: 2021-07-15.

[8] R. van den Hoed, S. Maase, J. Helmus, R. Wolbertus, Y. el Bouhassani, J. Dam, M. Tamis, and B. Jablonska, "E-mobility: getting smart with data," 2019.

[9] A. R. Abul'Wafa, A. El'Garably, and W. A. Mohamed, "Uncoordinated vs Coordinated Charging of Electric Vehicles in Distribution Systems Performance," *International Journal of Engineering and Information Systems (IJEAIS)*, vol. 1, pp. 54 – 65, Sept. 2017.

[10] Q. Wang, X. Liu, J. Du, and F. Kong, "Smart charging for electric vehicles: A survey from the algorithmic perspective," *IEEE Communications Surveys & Tutorials*, vol. 18, no. 2, pp. 1500–1517, 2016.

[11] R. Fachrizal, M. Shepero, D. van der Meer, J. Munkhammar, and J. Widén, "Smart charging of electric vehicles considering photovoltaic power production and electricity consumption: A review," *eTransportation*, vol. 4, p. 100056, 2020.

[12] C. Li, C. Liu, K. Deng, X. Yu, and T. Huang, "Data-driven charging strategy of pevs under transformer aging risk," *IEEE Transactions on Control Systems Technology*, vol. 26, no. 4, pp. 1386–1399, 2017.

[13] S. Yeo and D.-J. Lee, "Selecting the optimal charging strategy of electric vehicles using simulation based on users' behavior pattern data," *IEEE Access*, 2021.

[14] E. C. Kara, J. S. Macdonald, D. Black, M. Bérges, G. Hug, and S. Kiliccote, "Estimating the benefits of electric vehicle smart charging at non-residential locations: A data-driven approach," *Applied Energy*, vol. 155, pp. 515–525, 2015.

[15] C. Heilmann and D. Wozabal, "How much smart charging is smart?," *Applied Energy*, vol. 291, p. 116813, 2021.

[16] A. Bocca, Y. Chen, A. Macii, E. Macii, and M. Poncino, "Aging and cost optimal residential charging for plug-in evs," *IEEE Design & Test*, vol. 35, no. 6, pp. 16–24, 2017.

[17] N. Sadeghianpourhamami, N. Refa, M. Strobbe, and C. Develder, "Quantitive analysis of electric vehicle flexibility: A data-driven approach," *International Journal of Electrical Power & Energy Systems*, vol. 95, pp. 451–462, 2018.

[18] M. Zweistra, S. Janssen, and F. Geerts, "Large scale smart charging of electric vehicles in practice," *Energies*, vol. 13, no. 2, p. 298, 2020.

[19] C. Will and A. Schuller, "Understanding user acceptance factors of electric vehicle smart charging," *Transportation Research Part C: Emerging Technologies*, vol. 71, pp. 198–214, 2016.

[20] L. Buzna, P. De Falco, S. Khormali, D. Proto, and M. Straka, "Electric vehicle load forecasting: A comparison between time series and machine learning approaches," in *2019 1st International Conference on Energy Transition in the Mediterranean Area (SyNERGY MED)*, pp. 1–5, IEEE, 2019.

[21] Y. Kim and S. Kim, "Forecasting charging demand of electric vehicles using time-series models," *Energies*, vol. 14, no. 5, p. 1487, 2021.

[22] J. Huber, D. Dann, and C. Weinhardt, "Probabilistic forecasts of time and energy flexibility in battery electric vehicle charging," *Applied Energy*, vol. 262, p. 114525, 2020.

[23] L. Buzna, P. De Falco, G. Ferruzzi, S. Khormali, D. Proto, N. Refa, M. Straka, and G. van der Poel, "An ensemble methodology for hierarchical probabilistic electric vehicle load forecasting at regular charging stations," *Applied Energy*, vol. 283, p. 116337, 2021.

[24] V. Alvarez, S. Mazuelas, and J. A. Lozano, "Probabilistic load forecasting based on adaptive online learning," *IEEE Transactions on Power Systems*, vol. 36, pp. 3668 – 3680, Jul. 2021.

[25] T. Hong and S. Fan, "Probabilistic electric load forecasting: A tutorial review," *International Journal of Forecasting*, vol. 32, no. 3, pp. 914–938, 2016.

[26] M. Motz, J. Huber, and C. Weinhardt, "Forecasting bev charging station occupancy at work places," *INFORMATIK 2020*, 2021.

[27] T.-Y. Ma and S. Faye, "Multistep electric vehicle charging station occupancy prediction using mixed lstm neural networks," *arXiv preprint arXiv:2106.04986*, 2021.

[28] C. Bikcora, N. Refa, L. Verheijen, and S. Weiland, "Prediction of availability and charging rate at charging stations for electric vehicles," in *2016 International Conference on Probabilistic Methods Applied to Power Systems (PMAPS)*, pp. 1–6, IEEE, 2016.

[29] M. F. Shaaban, M. Ismail, E. F. El-Saadany, and W. Zhuang, "Real-time pev charging/discharging coordination in smart distribution systems," *IEEE Transactions on Smart Grid*, vol. 5, no. 4, pp. 1797–1807, 2014.

[30] K. L. López, C. Gagné, and M.-A. Gardner, "Demand-side management using deep learning for smart charging of electric vehicles," *IEEE Transactions on Smart Grid*, vol. 10, no. 3, pp. 2683–2691, 2018.

[31] Y.-W. Chung, B. Khaki, T. Li, C. Chu, and R. Gadh, "Ensemble machine learning-based algorithm for electric vehicle user behavior prediction," *Applied Energy*, vol. 254, p. 113732, 2019.

[32] Y. Chen, K. S. S. Alamin, D. Jahier Pagliari, S. Vinco, E. Macii, and M. Poncino, "Electric vehicles plug-in duration forecasting using machine learning for battery optimization," *Energies*, vol. 13, no. 16, p. 4208, 2020.

[33] Z. J. Lee, T. Li, and S. H. Low, "Acn-data: Analysis and applications of an open ev charging dataset," in *Proceedings of the Tenth ACM International Conference on Future Energy Systems*, pp. 139–149, 2019.

[34] A. S. Al-Ogaili, T. J. T. Hashim, N. A. Rahmat, A. K. Ramasamy, M. B. Marsadek, M. Faisal, and M. A. Hannan, "Review on scheduling, clustering, and forecasting strategies for controlling electric vehicle charging: challenges and recommendations," *IEEE Access*, vol. 7, pp. 128353–128371, 2019.

[35] S. Khan, B. Brandherm, and A. Swamy, "Electric vehicle user behavior prediction using learning-based approaches," in *2020 IEEE Electric Power and Energy Conference (EPEC)*, pp. 1–5, 2020.

[36] S. Shahriar, A. Al-Ali, A. H. Osman, S. Dhou, and M. Nijim, "Prediction of ev charging behavior using machine learning," *IEEE Access*, 2021.

[37] O. Frendo, N. Gaertner, and H. Stuckenschmidt, "Improving smart charging prioritization by predicting electric vehicle departure time," *IEEE Transactions on Intelligent Transportation Systems*, 2020.

[38] S. Shahriar, A. Al-Ali, A. H. Osman, S. Dhou, and M. Nijim, "Machine learning approaches for EV charging behavior: A review," *IEEE Access*, vol. 8, pp. 168980–168993, 2020.

[39] K. Miyazaki, T. Uchiba, and K. Tanaka, "Clustering to predict electric vehicle behaviors using state of charge data," in *2020 IEEE International Conference on Environment and Electrical Engineering and 2020 IEEE Industrial and Commercial Power Systems Europe (EEEIC/I&CPS Europe)*, pp. 1–6, IEEE, 2020.

[40] T. Lan, X. Liu, S. Wang, K. Jermsittiparsert, S. T. Alrashood, M. Rezaei, L. Al-Ghussain, and M. A. Mohamed, "An advanced machine learning based energy management of renewable microgrids considering hybrid electric vehicles' charging demand," *Energies*, vol. 14, no. 3, p. 569, 2021.

[41] A. Lucas, R. Barranco, and N. Refa, "Ev idle time estimation on charging infrastructure, comparing supervised machine learning regressions," *Energies*, vol. 12, no. 2, p. 269, 2019.

[42] S. Ai, A. Chakravorty, and C. Rong, "Household ev charging demand prediction using machine and ensemble learning," in *2018 IEEE International Conference on Energy Internet (ICEI)*, pp. 163–168, IEEE, 2018.

[43] X. Ge, L. Shi, Y. Fu, S. Muyeen, Z. Zhang, and H. He, "Data-driven spatial-temporal prediction of electric vehicle load profile considering charging behavior," *Electric Power Systems Research*, vol. 187, p. 106469, 2020.

[44] H. M. Abdullah, A. Gastli, and L. Ben-Brahim, "Reinforcement learning based EV charging management systems–a review," *IEEE Access*, vol. 9, pp. 41506–41531, 2021.

[45] M. Dabbaghjamanesh, A. Moeini, and A. Kavousi-Fard, "Reinforcement learning-based load forecasting of electric vehicle charging station using q-learning technique," *IEEE Transactions on Industrial Informatics*, vol. 17, no. 6, pp. 4229–4237, 2020.

[46] Y. B. Khoo, C.-H. Wang, P. Paevere, and A. Higgins, "Statistical modeling of electric vehicle electricity consumption in the victorian ev trial, australia," *Transportation Research Part D: Transport and Environment*, vol. 32, pp. 263–277, 2014.

[47] Y. Amara-Ouali, Y. Goude, P. Massart, J.-M. Poggi, and H. Yan, "A review of electric vehicle load open data and models," *Energies*, vol. 14, no. 8, 2021.

[48] N. Refa and N. Hubbers, "Impact of smart charging on evs charging behaviour assessed from real charging events," in *Proc. 32th Int. Electr. Vehicle Symp*, 2019.

[49] J. Wu, Y.-G. Wang, Y.-C. Tian, K. Burrage, and T. Cao, "Support vector regression with asymmetric loss for optimal electric load forecasting," *Energy*, vol. 223, p. 119969, 2021.

[50] J. Kim, H. Seung, J. Lee, and J. Ahn, "Asymmetric preference and loss aversion for electric vehicles: The reference-dependent choice model capturing different preference directions," *Energy Economics*, vol. 86, p. 104666, 2020.

[51] M. T. Kahlen, W. Ketter, and J. van Dalen, "Electric vehicle virtual power plant dilemma: Grid balancing versus customer mobility," *Production and Operations Management*, vol. 27, no. 11, pp. 2054–2070, 2018.

[52] C. X. Ling and V. S. Sheng, *Cost-Sensitive Learning*, pp. 231–235. Boston, MA: Springer US, 2010.

[53] G. Elliott and A. Timmermann, "Optimal forecast combinations under general loss functions and forecast error distributions," *Journal of Econometrics*, vol. 122, no. 1, pp. 47–79, 2004.

[54] C. Davino, M. Furno, and D. Vistocco, *Quantile regression: theory and applications*, vol. 988. John Wiley & Sons, 2013.

[55] S. Boyd and L. Vandenberghe, *Convex Optimization*. Cambridge University Press, March 2004.

[56] R. Koenker, *Quantile Regression*. Econometric Society Monographs, Cambridge University Press, 2005.

[57] G. James, D. Witten, T. Hastie, and R. Tibshirani, *An Introduction to Statistical Learning: with Applications in R.* Springer, 2013.

[58] T. Hastie, R. Tibshirani, and M. Wainwright, *Statistical Learning with Sparsity: The Lasso and Generalizations.* Chapman & Hall/CRC, 2015.

[59] T. Hastie, R. Tibshirani, and J. Friedman, *The Elements of Statistical Learning.* Springer Series in Statistics, New York, NY, USA: Springer New York Inc., 2001.

[60] M. Kuhn and K. Johnson, *Applied predictive modeling*, vol. 26. Springer, 2013.

[61] M. Straka, R. Carvalho, G. V. D. Poel, and v. Buzna, "Analysis of energy consumption at slow charging infrastructure for electric vehicles," *IEEE Access*, vol. 9, pp. 53885–53901, 2021.

[62] N. Sadeghianpourhamami, J. Deleu, and C. Develder, "Definition and evaluation of model-free coordination of electrical vehicle charging with reinforcement learning," *IEEE Transactions on Smart Grid*, vol. 11, no. 1, pp. 203–214, 2019.

[63] D. Hall and N. Lutsey, "Literature review on power utility best practices regarding electric vehicles," tech. rep., International Council On Clean Transportation, 2017. Available as: `https://theicct.org/sites/default/files/publications/Power-utility-best-practices-EVs_white-paper_14022017_vF.pdf`.

[64] J. Bergstra and Y. Bengio, "Random search for hyper-parameter optimization.," *Journal of machine learning research*, vol. 13, no. 2, 2012.

[65] ElaadNL, "Elaadnl." `https://www.elaad.nl/`, 2015. Accessed: 2021-06-25.

[66] Ibedrola, "Ibedrola charging plans." `https://www.iberdrola.es/en/smart-mobility/electric-vehicle-plan`, 2021. Accessed: 2021-11-10.

[67] E-flux, "E-flux charging rates." `https://www.e-flux.nl/en/e-flux-mobility-cards/charge-rates/`, 2021. Accessed: 2021-11-10.

[68] edockets, "edockets charging rates." `https://www.edockets.state.mn.us/EFiling/edockets/searchDocuments.do?method=showPoup&documentId=f60A5CA63-0000-C11E-9F24-C36F15592A04g&documentTitle=20186-143541-01`, 2021. Accessed: 2021-11-10.